AIAA 92-4714

Inverse Design of Super Elliptic Coolant Passages in Coated Turbine Blades With Specified Temperatures and Heat Fluxes

G.S. Dulikravich and T.J. Martin
The Pennsylvania State University
University Park, PA

Fourth
AIAA/USAF/NASA/OAI
Symposium on Multidisplinary Analysis and Optimizations
September 21-23, 1992 / Cleveland, OH

INVERSE DESIGN OF SUPER ELLIPTIC COOLANT PASSAGES IN COATED TURBINE BLADES WITH SPECIFIED TEMPERATURES AND HEAT FLUXES

George S. Dulikravich* and Thomas J. Martin**
Department of Aerospace Engineering, The Pennsylvania State University
University Park, PA 16802, USA

Abstract

A highly accurate and reliable algorithm capable of performing automatic inverse design of coolant flow passage numbers, shapes, sizes and locations inside coated solid objects has been developed. The user has the freedom to specify arbitrary temperatures and heat fluxes at the points on the outer surface of the object and either temperatures or heat fluxes on the surfaces of the yet unknown coolant flow passages. The number of passages required could be guessed and the algorithm will automatically eliminate the unnecessary passages. The method allows even inexperienced designers to achieve an optimal configuration of coolant passages in a single computer run while satisfying user-specified manufacturing constraints that were incorporated via a barrier function method. The optimization algorithms used in this inverse design code were based on gradient search and on a modified Newton search. A simple method for escaping from local minima has been implemented that involves switching between two different formulations of the objective function. The optimal value of the gradient search parameter was found using a simple method of fitting a highly accurate spline through a set of points in the cost function/search parameter plane and seeking out the value that will generate minimal error.

I. Background

The design of internally cooled turbine blades is usually accomplished using approximate empirical methods, repetitive numerical analysis of intuitively modified coolant passage configurations and expensive experimentation. In this approach, the proper number, dimensions, shapes and locations of the coolant passages (holes) are usually determined according to the designer's experience. The development of high speed computers and adequate numerical techniques has made it possible to approach the design problem differently and to solve it more efficiently and accurately.

The mathematical model for steady heat conduction in coated turbine blades is represented by the boundary value problem for Laplace's equation over a multiply-connected domain. For a given two-dimensional outer boundary shape, the temperature is specified on both the inner (hole) and outer (blade hot surface) boundary as is the initial guess for the number, locations, shapes and sizes of coolant holes inside the blade. The goal is to determine the minimum necessary number and the proper locations, shapes and sizes of the holes, such that the relative error between the specified and computed heat fluxes at the outer boundary is minimized. Specifying heat fluxes on the outer (hot) surface in addition to the already specified temperature distribution along the same surface creates an over-specified boundary value problem. Such an over specified problem can be solved by an inverse (design) approach where the number, locations, shapes, and sizes of the holes are readjusted appropriately. These parameters can be determined using an optimization technique. The first application of such inverse methodology and an optimization techniques in solving the design problem for turbine blade coolant flow passages was reported by Kennon and Dulikravich[1-3]. Their objective function was defined as a relative error between the specified heat fluxes on the outer (hot) boundary and the computed heat fluxes obtained by analyzing the temperature field for the current configuration of holes. Since an analytical solution to the boundary value problem for Laplace's equation governing a steady temperature field in an irregular multiply-connected domain does not exist, the Boundary Element Method (BEM)[4] was used for its numerical integration. The BEM was chosen due to its simplicity, accuracy and geometric flexibility and because it requires substantially less computing time than the finite element method or the finite difference method. Specifically, it does not require a repetitive costly two-dimensional computational grid generation for multiply connected domains. The objective function was minimized using the Fletcher-Reeves gradient search method[5].

Since then, this inverse design procedures for the optimization of coolant flow passages in turbine blades has been constantly improved. For example, inverse design of the passages in blades with ceramic coating[6] implicitly guarantees minimal temperature gradients throughout the structure. In addition to the specified heat flux on the outer surface, the turbine blade design was also made to satisfy two manufacturing constraints: minimum allowable distance between neighboring holes as well as minimum allowable distance between any hole and the outer boundary (or blade/coating interface if the blade is coated). A summary of methodologies for inverse (design) problems in steady and unsteady heat conduction was published by Dulikravich[7].

---

* Associate Professor. Associate Fellow AIAA.

** Graduate Assistant. Student member AIAA.

More recently [8], the inverse (design) problem of minimizing the number of necessary coolant flow passages having circular cross sections in addition to their proper dimensions (radii) and locations when temperature is specified on the outer (hot) surface and on the unknown, inner (cold) surface has been accomplished. Cross sections of the coolant flow passages were chosen to be circular since, from the manufacturing point of view, circular shapes are more desirable than arbitrary shapes[1-3]. This effort was then extended[9-11] to allow for coolant flow passages having cross sections that belong to a family of inclined Lame curves (super elliptic functions) of the general form

$$\left[\frac{x - x_0}{a}\right]^n + \left[\frac{y - y_0}{b}\right]^n = 1 \qquad (1)$$

Here, coordinates x_0 and y_0 of the center of a super elliptic hole, hole semi-axis a and b, Lame curve exponent n, and the angle θ of inclination of the local coordinate system x, y with respect to the global coordinate system x', y' could be used as design variables[9-11]. This formulation provides more control over the shape of the hole since the exponent n allows for shapes varying smoothly from star-shaped (n < 1), to circular (a=b, n=2) or elliptic (a>b, n=2) to square or rectangular ($n \rightarrow \infty$). Thus, the shapes of the holes can vary significantly, while requiring only six parameters (x_0, y_0, a, b, n, θ) per hole to be optimized. It should be noted that the shapes of the holes should be defined not only from the manufacturing point of view, or by the requirements of heat conduction through the turbine blade, but also by the heat convection inside the coolant passage. This topic requires a fully three-dimensional extension of this design methodology and will not be addressed in the present work.

II. The Optimization Technique

The complexity of the given inverse (design) problem requires the use of a relatively simple but robust and fast optimization technique for constrained nonlinear optimization. The Davidon-Fletcher-Powell (DFP)[5,12] algorithm combined with the barrier function method[12] was implemented[6-11] because it requires a relatively low number of objective function evaluations, which is the most expensive part of optimization in terms of computing time. The DFP method approximates the Hessian matrix so that second order partial derivatives do not have to be computed directly. Using the barrier function method it is possible to include constraints in the objective function so that constraint functions and their gradients do not have to be computed. This approach, though, can cause convergence to become quite slow. A first order numerical approximation (first order accurate one-sided finite differencing) was used to compute gradients of the objective function.

Since the number of holes is a design variable, the problem arises from the fact that this is the only discrete variable in the design vector. It is not a regular design variable because each of the initially guessed holes can be over specified and when computing the gradient of the objective function all the possible combinations should be taken into account. Moreover, the number of holes can be underestimated initially as it will be demonstrated in the last test case in this paper. The most general algorithm should allow for increasing the number of holes, as well. The question is where such new holes should be introduced and what should be their configurations. A simpler and more straightforward approach is to start optimizing with the highest possible number of holes (which is limited by the computer memory available) and then reduce the number of holes during the optimization procedure to a number which minimizes the objective function and satisfies all the constraints. The criterion for excluding a particular hole or holes from further optimization, and thus reducing the design vector by six design variables per each excluded hole, must be specified by the user. It can be defined as a percentage of the characteristic dimension of the problem. For example, it can be a small fraction of the chord length in the case of a turbine blade. Obviously, when the size of a hole becomes very small, its influence on the solution also becomes negligible. Instead of wasting computational time on recomputing the entire solution, we can eliminate any hole that is reduced beyond a pre-specified size. Otherwise, the procedure is time consuming, it often terminates in a local minimum, and the obtained solution is not fully converged[8].

II.1 Objective Function Switching

Optimization techniques require the highest possible accuracy of the analysis computer code[6]. Due to local minima that can occur in the objective function and due to truncation error the code sometimes stalls before achieving an optimal solution. In order to overcome such a situation a new technique has been devised[8]. In this approach, whenever the optimization stalls, the formulation of the objective function is automatically changed. The new objective function provides a departure from a local minimum and further convergence towards the global minimum.

Specifically, the objective to minimize the difference between the specified and the calculated heat flux at the outer boundary can be expressed in more than one way. In this work two different definitions of the objective function were used. The difference between the specified heat flux and the heat flux obtained from the current configuration is mathematically formulated as an L_2 norm. The objective function F can be computed as a global error (error in total heat flux through the blade outer boundary)

$$F_1(x) = \frac{\sum_{j=1}^{N_{hot}} (q_{hot}^{spec} - q_{hot}^{calc})_j^2}{\sum_{j=1}^{N_{hot}} (q_{hot}^{spec})_j^2 + \varepsilon} \times 100 \qquad (2)$$

or as a local normalized error in the heat flux at each panel j of the hot surface

$$F_2(x) = \sum_{j=1}^{N_{hot}} \left[\frac{(q_{hot}^{spec} - q_{hot}^{calc})^2}{(q_{hot}^{spec})^2 + \varepsilon}\right]_j \times 100 \qquad (3)$$

Here, N_{hot} is the total number of panels on the blade hot (outer) surface, q_{hot}^{spec} is the specified (desired) heat flux and q_{hot}^{calc} is the computed heat flux at the outer (hot) surface of the blade, and ε is a small user-specified parameter. For example, we used ε = 1.0e-6.

II.2 Constraints and Barrier Function

The two manufacturing constraints were incorporated into the objective function using a barrier function of the following form

$$B(g(x)) = C\,F_n(x) \sum_{m=1}^{M} \sum_{i=1}^{N_m} \left[\sum_{k=1}^{N_k} \frac{d^s}{\left(D_{ik}^s - d^s\right)} + \sum_{l=1}^{N_l} \frac{d^h}{\left(D_{il}^h - d^h\right)} \right] \quad (4)$$

Here, M is the total number of holes, N_m is the number of panels on hole m, N_k is the number of panels on the interface between the blade and the coating, and N_l is the number of panels on the hole l. Here, D_{ik}^s is the current distance between the panel i on the hole m and the panel k on the interface between the core of the blade and the blade coating. Similarly, D_{il}^h is the current distance between the panel i on the hole m and the panel l on a different hole. The weighting function $C\,F_n(x)$ is initially large and then gradually decreases so that with each optimization cycle the influence of the barrier function decreases. Here, the parameter $C < 1$ is a user specified value. The barrier function is established so that it has a singular value when the constraints are violated and it is a rapidly growing function as long as the imposed constraints are nearly violated. It should be emphasized that every element in the sum given by the formula above (Eq. 4) must be non-negative. If any element becomes negative, this means violation of the constraints. In that case the optimization process is stopped and computation of gradients is restarted using new spatial differences Δx and Δy. It was possible to use the barrier function in this problem since non-equality type constraints are involved. The most important advantage of the barrier function is that it incorporates the constraints in the objective function. Thus, it always iterates through the feasible region and gives a feasible design. Finally, the composite objective function can have two forms

$$\tilde{F}_n(g(x)) = F_n(x) + B(g(x)) \qquad n = 1, 2 \quad (5)$$

depending whether a global or a local objective function is used for its evaluation.

II.3 Optimum Line Search Parameter

It has been observed[7] that these types of optimization problems often have minimas of a "crevice" type, that is, the global minima are hard to detect because they occur over a very narrow range of line search parameters, α. Moreover, the optimal values of α often border on values of α that give a sharp rise in the composite error (objective function). Standard techniques (golden section, Fibonacci method, quadratic or cubic fitting, etc.) often do not work well or not at all[13] on these types of problems with narrow minimas. Consequently, we have used here a method described by Dulikravich[7] that is based on spline fitting and interpolation. In particular, composite objective functions for, say, six equally spaced values of α in the interval $0 < \alpha < 1$ are initially computed. A highly accurate exponential spline is then numerically fitted through these values of $\tilde{F}_n(g(x))$ and interpolated at , say, 1000 equidistantly spaced values of α in the same interval $0 < \alpha < 1$. A simple search is then conducted to find α^*, that is, an optimum value of α that will produce a minimum value of $\tilde{F}_n(g(x))$ during the next optimization cycle. After α^* is actually implemented in the line search DFP algorithm, it will produce a certain value of the composite error, $\tilde{F}_n(g(x))$. This value will be now added to the initial set of six points thus creating a more complete set consisting of seven $\tilde{F}_n(g(x))$, α pairs. The exponential spline will now be fitted through the original six points plus this new point and then interpolated at 1000 equidistantly spaced values of α in the interval $0 < \alpha < 1$. A new, improved value of α^* will be determined using a simple search and the entire procedure will be repeated. Typically, it suffices to use about ten such cycles before the change in composite objective functions resulting from two consecutively evaluated α^* becomes negligible indicating a truly optimal α^* for this optimization cycle.

In summary, the optimization procedure consists of the following steps:

(1) Specify the shape of the outer (hot) surface and the coating of the turbine blade.

(2) Specify the desired temperature distribution on the outer (hot) surface and the inner (hole) surfaces.

(3) Specify the desired heat flux distribution on the outer (hot) surface. In practice, hot surface heat flux is obtained as a by-product of the hot flow field computations around the blade when its hot surface temperature is specified.

(4) Specify manufacturing constraints:
(i) minimum distance between holes and the metal/coating interface, and
(ii) minimum distance between any two holes.

(5) Specify an initial guess for the number of holes (M), their sizes (a_m, b_m), shapes (n_m), locations of

their centers (x_{0m}, y_{0m}), and their inclinations (θ_m). Thus, if there are M holes, there will be 6 × M design variables.

(6) Using the BEM, the Dirichlet boundary value problem (specified temperatures on the blade outer surface and on the surfaces of the guessed holes) for Laplace's equation is solved. Heat fluxes through the outer boundary are computed and composite objective functions are formed. The gradient of the composite objective function is computed using finite differences. Laplace's equation is solved 6 × M times, once for each design variable on each of the holes, in order to compute the gradient. To find a feasible design which minimizes the composite objective function in the direction of the gradient, different values of the search parameter α, which multiplies the gradient of the composite objective function, have to be found. The value of α which gives the minimal value of $\tilde{F}_n$ is determined using repetitive exponential spline fitting and interpolation and then used to update the design variables.

(7) Use the DFP technique to find the new values of design variables repeating the optimization procedure from step (6) until the variation of the corresponding composite objective function $\tilde{F}_n$ is below the value specified as the convergence criterion. If the dimension of one of the holes becomes less than the prespecified small value, the hole is eliminated from further optimization procedure. If the optimization procedure stalls in a local minimum, the objective function formulation is changed from Eq. 2 to Eq. 3 while continuing with optimization from step (6).

III. Boundary Element Formulation

It is assumed that the temperature field is already steady and that the solid material of the internally cooled configuration is thermally isotropic. Thermal expansion is neglected. Consequently, the governing energy equation is simply Laplace's equation

$$\nabla^2 T = 0 \quad \text{in} \quad \Omega, \tag{6}$$

In this work the BEM was applied. Instead of starting with the differential form of the boundary value problem for Laplace's equation and the boundary condition

$$T = \bar{T} \quad \text{on} \quad \Gamma_m \tag{7}$$

where ∇^2 represents Laplace's operator, Ω denotes domain, and Γ_m is the m-th part of its boundary, the starting point is the integral form

$$\int_\Omega \nabla^2 (T - \bar{T})\, \tilde{w}\, d\Omega = 0 \tag{8}$$

where Laplace's equation is multiplied by a function $\tilde{w}$, continuous up to the second order. It should be noted that the boundary conditions are now incorporated in the equation itself. After integrating by parts twice and introducing the fundamental solution T^* instead of the function $\tilde{w}$, the equation can be written as

$$\int_\Omega (\nabla^2 T)\, T^*\, d\Omega = \int_{\Gamma_1} (q - \bar{q})\, T^*\, d\Gamma - \int_{\Gamma_2} (T - \bar{T})\, q^*\, d\Gamma \tag{9}$$

where Γ_1 is the boundary on which heat flux $\bar{q}$ is specified and Γ_2 is the boundary on which temperature $\bar{T}$ is specified. The fundamental solution for using heat source surface singularities is

$$T^* = \frac{1}{2\pi} \ln \frac{1}{r} \tag{10}$$

where r is the distance from the point of observation to the surface panel point under consideration. The derivative of the fundamental solution normal to the boundary is

$$q^* = \frac{\partial T^*}{\partial n} \tag{11}$$

where n is the direction normal to the boundary. After integrating by parts once more and substituting for q^*, the final form of the integral equation is obtained as

$$c_j T_j + \int_\Gamma T\, q^*\, d\Gamma = \int_\Gamma T^*\, q\, d\Gamma \tag{12}$$

where T_j is the temperature of the j-th point on the boundary. Here,

$$c_j = \frac{\theta_j}{2\pi} \tag{13}$$

where θ_j is the internal angle of the corner between two neighboring panels expressed in radians.

The integral equation can be discretized by discretizing boundary Γ into a series of linear elements and assuming linear variations of T and q over each particular element. However, the distribution of T and q over an element can be arbitrary. For the sake of simplicity and efficiency, the use of locally linear variations gives a sufficiently accurate solution. Then the discretized integral equation takes the following form

$$c_i T_i = \sum_{k=1}^{2N} G_{ik}\, q_k - \sum_{l=1}^{N} \bar{H}_{il}\, T_l \tag{14}$$

where N is the total number of boundary element nodes and i is the running index of the surface nodes. Here,

diagonals of the matrix $\bar{H}$ are computed implicitly[4] rather than by calculating the interior angles at the corners between the neighboring panels. Introducing

$$H_{ii} = -\sum_{l=1}^{N} \bar{H}_{il} \quad \text{if } l \neq i \tag{15}$$

equation (14) can be written as

$$\sum_{l=1}^{N} H_{il} T_l = \sum_{k=1}^{2N} G_{ik} q_k \tag{16}$$

Once all the unknowns are placed on the left hand side to form a vector **X** and matrices **H** and **G** are rearranged to form a new matrix, this new system of linear algebraic equations can be solved for vector **X** by Gauss elimination

$$\mathbf{A\ X = B} \tag{17}$$

The problem of possible non-uniqueness of the solution to integral formulation (Eq. 9), assuming a fundamental solution of the form given by (Eq. 10), can be avoided by scaling the entire domain so that the maximal dimension is less then one[6].

IV. Results

IV.1. Coated Hollow Disk

This test case was used to evaluate the accuracy of the BEM code with sequentially varying boundary conditions and to demonstrate the hole elimination capability. The geometry consisted of a circular disk (radius 1.2m) with a centrally located circular hole (radius 0.5m). The disk was coated with the coating occupying the region 0.9m < r < 1.2m. The ratio of thermal conductivities of the coating and the disk core region was 1:5. The outer surface of the disk and the interface between the disk core and the coating were discretized using 36 equal-length flat panels, respectively. The wall of the centrally located circular hole was discretized using 20 equal-length flat panels. The BEM code was first run with a constant temperature T_{hot}^{spec} = 100 K specified on the outer surface (radius 1.2m) and a constant temperature T_{cold}^{spec} = 50 K on the inner surface (a circular hole of radius 0.5m). The computed heat fluxes on the outer and the inner surface were then used as Neuman boundary conditions on the parts of the outer boundary and the circular hole. Specifically, the boundary condition specified on the upper half of the outer circular surface was the uniform computed radial temperature gradient (q_{hot}^{spec} = 103 K/m), while on the lower half of the outer circular surface a uniform original temperature (T_{hot}^{spec} = 100 K) was enforced. At the same time, the computed constant radial temperature gradient (q_{cold}^{spec} = -250 K/m) was specified on the left wall ($3\pi/2 > \theta > \pi/2$) of the centrally located circular hole hole, while the original uniform temperature (T_{cold}^{spec} = 50 K) was specified on the right wall ($\pi/2 > \theta > -\pi/2$) of the hole. When the numerical results obtained with the BEM code for this sequentially varying boundary conditions were compared with the locally analytical solutions for the heat flux and temperature, the BEM routine was found to be highly accurate: it had only 0.03% error versus the analytic solution.

The first test case involving optimization was then created by introducing three holes (Fig. 1) instead of a single centrally located circular hole. The three holes of various super elliptic shapes (an ellipse, a square and a rounded rectangle) were used as an initial guess for the configuration which in reality should have only a single centrally located circular hole (Fig. 2). Values of the design variables for the initial three holes are summarized in Table 1.

a	b	n	x_o	y_o	θ
0.4	0.2	2.0	-0.4	0.0	90.
0.2	0.2	1.0	0.4	0.4	0.
0.3	0.2	6.0	0.2	-0.4	0.

TABLE 1. Case 1: Initial design variables

The boundary conditions on the surfaces of the three guessed holes were: a constant radial temperature gradient q_{cold}^{spec} = -250 K/m was specified on the left wall ($3\pi/2 > \theta > \pi/2$) of each hole, while a constant temperature T_{cold}^{spec} = 50 K was specified on the right wall ($\pi/2 > \theta > -\pi/2$) of each hole . On the upper half of the outer disk surface a uniform temperature gradient (q_{hot}^{spec} = 103 K/m) was specified, while enforcing the uniform temperature (T_{hot}^{spec} = 100 K) on the lower half of the outer disk surface. The composite objective functions for the optimization procedure used in this test case were a combination of the composite objective functions based locally either on temperatures or on heat fluxes. The DFP optimization algorithm reached the fully converged solution (single, centrally located circular hole of 0.5m radius) in 99 optimization cycles. It eliminated the third hole after 17 cycles and the first hole after 45 optimization cycles. Figure 3 shows some of the intermediate hole configurations during the optimization process. The dotted lines indicate intermediate geometries and the solid line is the final and fully converged geometry. Notice that the initially square-shaped hole dominated and eventually turned circular after the other two holes collapsed to needle-shaped objects. Figure 4 depicts the convergence history of the composite objective function where the spikes occur due to three reasons:

1. Automatic composite objective function switching from global to local (Eqs. 2 and 3) and vice versa, since

the local composite objective function is always larger than the global composite objective function.
2. Hole elimination causes a jump in the composite objective function. If the holes were allowed to shrink to an extremely small size, this jump would not occur. Nevertheless, the computer time for achieving this would be unjustifiably large.
3. The program is made to stop if the composite cost function switching is performed during two consecutive optimization cycles indicating the inability of the algorithm to escape the local minima. In this case, the design variables are user-perturbed and then the program resubmitted.

The entire optimization procedure required 2269 calls to the BEM analysis routine and consumed 2790 seconds of CPU time on an IBM 3090.

IV.2 Coated Turbine Blade

We used a realistically shaped turbine blade having a chord length of 0.083 m and the coating thickness 0.5% of the chord. The thermal conductivities were 1.0 W/m K for the coating and 23.0 W/m K for the metal core material of the blade thus making the ratio of thermal conductivities 1:23. It was assumed that the coated blade has three interior coolant flow passages and that their shapes, sizes and locations are as depicted in Figure.5 and in Table 2 where the values of a, b, x_0 and y_0 are given in meters.

a	b	n	x_0	y_0	θ
0.005	0.005	2	-0.02	-0.0075	0
0.005	0.005	2	-0.01	-0.0075	0
0.005	0.005	2	0.00	-0.0075	0

TABLE 2. Case 2: Initial design variables

All boundary conditions were of the Dirichlet type with a realistic variation of temperature specified on the outer (hot) surface (Fig. 5) and a constant temperature T = 500 K specified on the coolant flow passage walls. The outer (hot) surface of the blade and metal/coating interface surface were discretized with 48 flat panels each. The surface of each of the three coolant flow passages (Fig. 5) was discretized with 20 flat panels. The panels were everywhere clustered with respect to the local surface curvature. In addition, a minimum distance of 0.0005 m between any of the holes and between the holes and the metal/coating interface were specified as the manufacturing constraints. The design variables for the fully converged geometry are listed in Table 3 and the target heat flux is shown in Figure 6.

a	b	n	x_0	y_0	θ
0.0075	0.0050	2	-0.0275	-0.0025	-40
0.0100	0.0075	6	-0.0075	-0.0100	0
0.0125	0.0050	2	0.0275	0.0100	55

TABLE 3. Case 2: Fully converged design variables

Figure 7 depicts the geometric evolution history at several stages during the optimization process. The optimization was completed when the normalized hot surface heat flux error (using the global cost function formulation and barrier function) reached 1.32 %. The dotted shapes indicate the intermediate geometries and the solid shapes indicate the final solution (not fully converged). Notice that each of the initially circular three holes transformed its shape appropriately and moved from their initial positions to the almost correct target configuration which would have been eventually reached by continuing the optimization process and further reducing the composite cost function. The entire optimization in this test case consumed 103 optimization cycles, 2859 calls to the BEM analysis routine, and 12,028 seconds of CPU time on an IBM 3090 computer.

IV.3 Increased Coolant Temperature

Assume now that a thermal systems designer wishes to use warmer high pressure air from the last stages of the high pressure compressor to cool the blades. This means an increase in the temperature of the coolant passage walls from, say, 500 K to 600 K. Also assume that the current values of the outer (hot) surface temperatures and heat fluxes are to be retained because of their direct influence on the aerodynamic performance of the blade. The objective is to examine if the previously optimized three-hole configuration (Fig. 6) with hole temperatures T = 500 K will be sufficient for the new, more extreme requirements of the holes with their surface temperatures T = 600 K. The initial guess (being the converged solution of the previous run with the hole temperatures T = 500 K) and the intermediate configurations of the holes are shown in Figure 8 as dotted shapes, while the final shapes of the holes are depicted with solid lines. Figure 9 shows the convergence history of the optimization process indicating that the process terminated at a local minima after the 12th optimization cycle. Composite objective function switching was performed automatically from global to local after the 2nd cycle and vice versa after the 8th cycle. Notice that the local composite objective function was more effective than the global as the hot surface normalized heat flux error reduced only about 2% with the global formulation and 9% with the local formulation. Unfortunately, the global error in the hot surface heat flux only reduced from 32% to 30% indicating that it is unlikely that a different constrained configuration with only three holes will allow for such a large increase in the temperature of the cooling fluid. In other words, the significantly warmer coolant in this instance requires a larger number of coolant flow passages in order to achieve the desired hot surface temperatures and heat fluxes.

V. Suggestions for Future Research

Future research in the field of inverse design of coolant flow passages in internally cooled configurations should be directed toward the development of multi-disciplinary, complex design tools which would include fluid flow analysis involving thermal convection, radiation and conduction as well as thermal stress-deformation field analysis and structural vibrations.

The computer code based on the optimization algorithm presented here is not vectorized. Due to the nature of the problem and the BEM approach, which results in a large system of linear algebraic equations with fully populated matrices, it is not possible to fully vectorize the computational procedure in order to increase the computational speed. This problem can be solved by either employing different numerical methods to solve Laplace's equation or by implementing

vectorization to the BEM. The latter goal can be achieved at the expense of a large amount of computer memory.

The same optimization procedure can be used for a variety[10] of practical problems governed by Laplace's partial differential equation. Faster and more reliable optimization packages can be readily substituted for the DFP routine. Specifically, we found that a quadratic programming algorithm of Pshenichny[14] required considerably fewer iteration cycles and consumed only a third of the computer time as compared to the DFP routine.

It is possible to approach an inverse design problem from a different point of view, besides the one presented in this work. A novel approach to the inverse design of coolant passages in turbine blades would be control theory approach. It has been shown recently that the control theory (adjoint operator)[15] approach to inverse design problems can efficiently lead to optimal solutions when optimizing a large number of variables. Finally, this method for inverse design is directly applicable and should be extended to fully three-dimensional arbitrary configurations.

VI. Acknowledgements

Authors are thankful to Mr. Scott G. Sheffer for correcting the grammar in this paper and helping with the optimization algorithm of Pshenichny and Danilin. Graphics and word processing were performed on the equipment donated by Apple Computers, Inc.

VII. References

1. Kennon, S.R., and Dulikravich, G.S., The Inverse Design of Internally Cooled Turbine Blades, *ASME Journal of Engineering for Gas Turbines and Power*, pp. 123-126, January 1985.

2. Kennon, S.R. and Dulikravich, G.S., Inverse Design of Multiholed Internally Cooled Turbine Blades, *International Journal of Numerical Methods in Engineering*, vol. 22, pp. 363-375, 1986a.

3. Kennon, S.R. and Dulikravich, G.S., Inverse Design of Coolant Flow Passages Shapes With Partially Fixed Internal Geometries, *International Journal of Turbo & Jet Engines,* vol. 3, (1), pp. 13-20, 1986b.

4. Brebbia, C.A. and Dominguez, J., Boundary Elements: An Introductory Course, McGraw-Hill Book Company, 1989.

5. Vanderplaats, G.N., Numerical Optimization Techniques for Engineering Design, McGraw-Hill, New York, 1984.

6. Chiang, T.L. and Dulikravich, G.S., Inverse Design of Composite Turbine Blade Circular Coolant Flow Passages, *ASME Journal of Turbomachinery*, vol. 108, pp. 275-282, 1986.

7. Dulikravich, G.S., Inverse Design and Active Control Concepts in Strong Unsteady Heat Conduction, *Applied Mechanics Reviews,* vol. 41, No. 6, June 1988, pp. 270-277, 1988.

8. Dulikravich, G.S. and Kosovic, B., Minimization of the Number of Cooling Holes in Internally Cooled Turbine Blades, *ASME paper 91-GT-103,* ASME Gas Turbine Confer., Orlando, FL, June 2-6, 1991; also *Internat. Journal of Turbo & Jet Engines*, 1992.

9. Dulikravich, G.S., Inverse Design of Proper Number, Shapes, Sizes and Locations of Coolant Flow Passages, *Proceedings of the 10th Annual CFD Workshop*, Editor: R. Williams, NASA MSFC, Huntsville, AL, April 28-30, 1992.

10. Dulikravich, G.S. and Martin, T.J., Determination of Void Shapes, Sizes and Locations Inside an Object With Known Surface Temperatures and Heat Fluxes, *Proceedings of the IUTAM Symposium on Inverse Problems in Engineering Mechanics,* Editors: M. Tanaka and H.D. Bui, Tokyo, Japan, May 11-15, 1992.

11. Dulikravich, G.S. and Martin, T.J., Determination of the Proper Number, Locations, Sizes and Shapes of Superelliptic Coolant Flow Passages in Turbine Blades, *Proc. of the Internat. Symp. on Heat and Mass Transfer in Turbomachinery (ICHMT),* Editor: R.J. Goldstein, Athens, Greece, Aug. 24-28, 1992.

12. Arora, J. S., Introduction to Optimum Design, McGraw-Hill Book Company, 1989.

13. Dulikravich, G.S. and Hayes, L.J., Control of Surface Temperatures to Optimize Survival in Cryopreservation, ASME Winter Annual Meeting, *Proceedings of the Symposium on Computational Methods in Bioengineering*, Editors: R.L. Spilker and B.R. Simon, BED-Vol.9, pp. 255-265, Nov. 27 - Dec.2, 1988.

14. Pshenichny, B. N and Danilin, Y. M., Numerical Methods in Extremal Problems, MIR Publishers, Moscow, 1969.

15. Tortorelli, D.A., A Systematic Approach for Shape Sensitivity Analysis, *AIAA paper 93-656*, Aerospace Sciences Meeting, Reno, NV, January 1993.

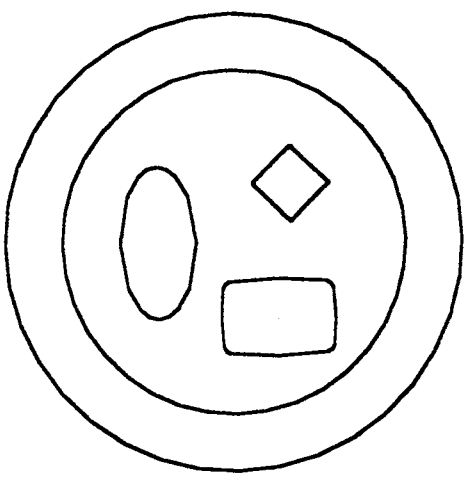

Figure 1. Coated circular disk: initial configuration consisting of three super elliptic holes (a square, an ellipse and a rounded rectangle)

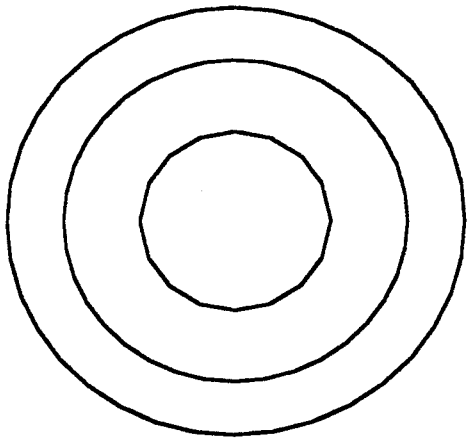

Figure 2. Coated circular disk: correct target configuration

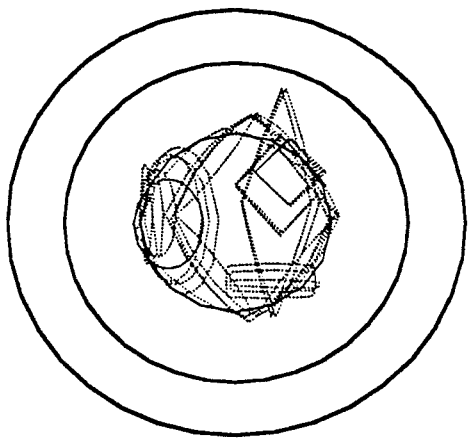

Figure 3. Coated circular disk: final hole configuration (solid line) and their intermediate shapes (dotted lines), Two unnecessary holes (ellipse and a rectangle) were automatically reduced to zero.

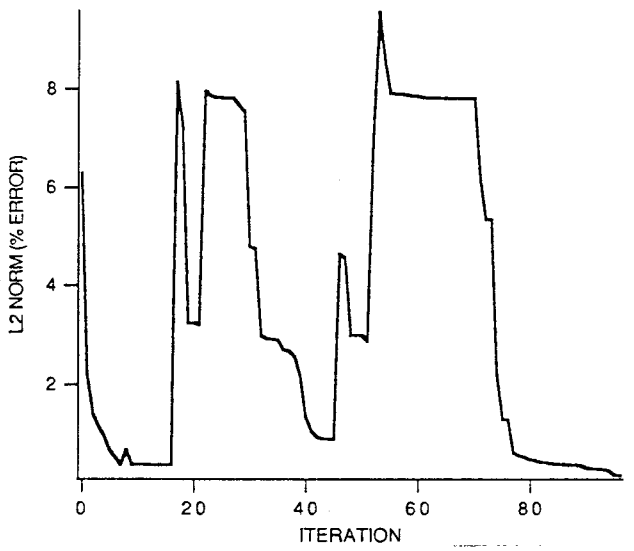

Figure 4. Coated circular disk: convergence history (percentage of the integrated heat flux error on the outer boundary versus number of optimization cycles).

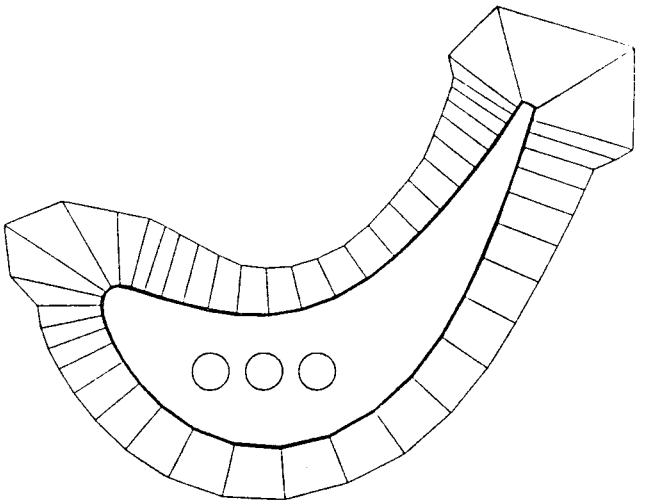

Figure 5. Coated turbine blade: specified temperature distribution on the blade outer (hot) surface and the initial hole configuration (three circles).

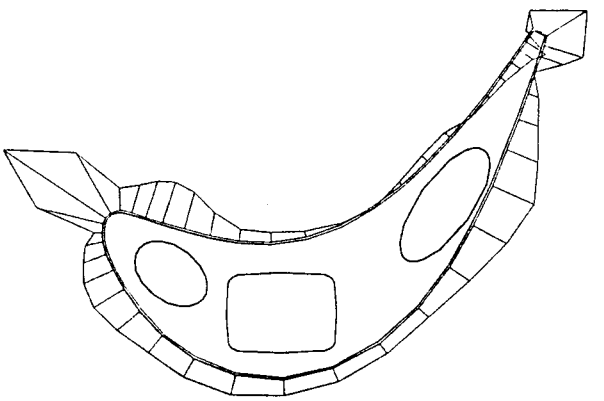

Figure 6. Coated turbine blade: specified heat flux distribution on the blade outer (hot) surface and target three-hole configuration with T=500 K on each hole.

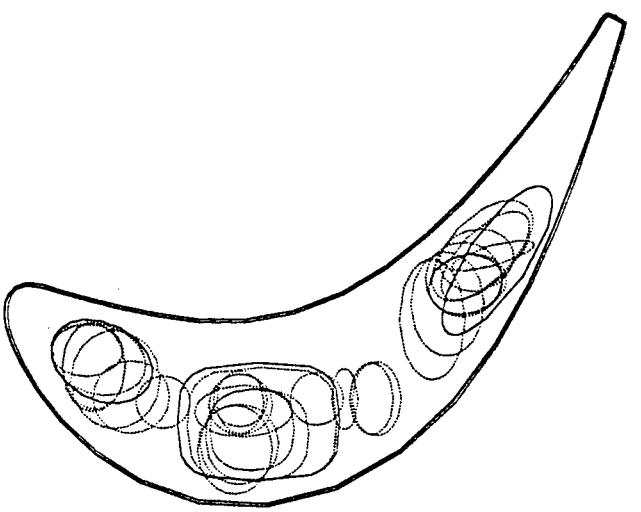

Figure 7. Coated turbine blade: geometric convergence history consisting of intermediate super elliptic hole shapes (dotted lines) and the converged configurations (solid lines) with T=500 K on each hole.

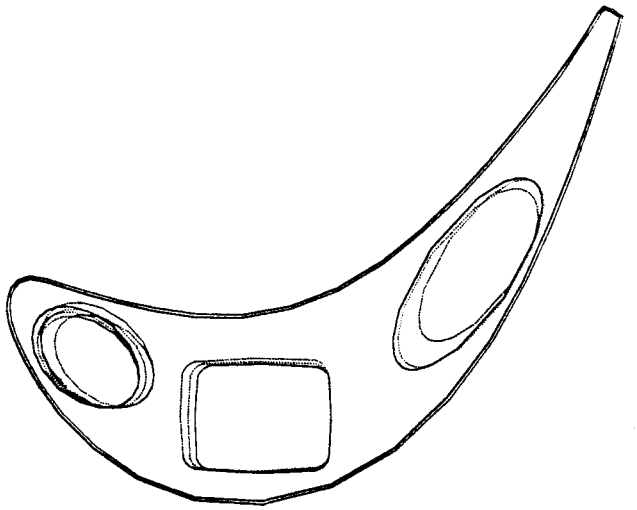

Figure 8. Coated turbine blade with T=600 K on each hole: intermediate shapes (dotted line) and the optimized configuration (full line) for the three holes with

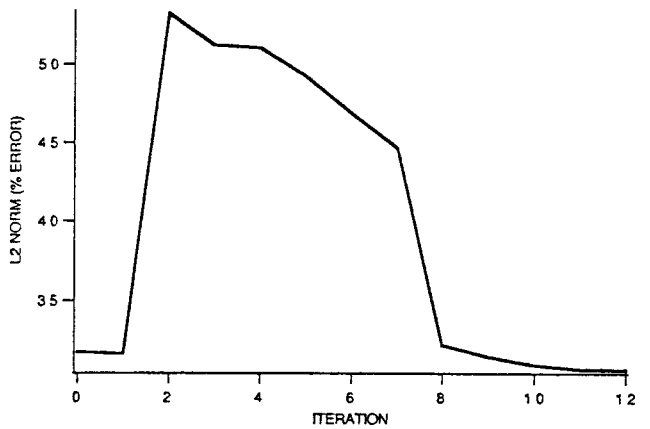

Figure 9. Coated turbine blade with T=600 K on each hole: convergence history (percentage of the integrated heat flux error on the outer boundary versus number of optimization cycles).